Transactions of the Materials Research Society of Japan 30[2] 531-534 (2005)

Analysis of carrier density and mobility for polycrystalline Bi without assuming intrinsic conditions

Y. Ishikawa[1], Y. Hasegawa[1], H. Shirai[2], H. Morita[3] and T. Komine[4]

[1]Graduate school of Science and Engineering, Saitama University, 338-8570, Japan
Phone: 81-48-858-3757, Fax: 81-48-858-3757, e-mail: ishikawa@kan.env.gse.saitama-u.ac.jp
[2]Department of Functional Materials Science, Saitama University, 338-8570, Japan
Phone: 81-48-858-3676, Fax: 81-48-858-3676, e-mail: shirai@fms.saitama-u.ac.jp,
[3]Saitama Industrial Technology Center, Saitama Prefecture, 333-0844, Japan
Phone: 81-48-265-1314, Fax: 81-48-265-1314, e-mail: morihiro@saitec.pref.saitama.jp,
[4]Department of Media and Telecommunications Engineering, Ibaraki University, 316-8511, Japan
Phone: 81-294-38-5118, Fax: 81-294-38-7148, e-mail: komine@mx.ibaraki.ac.jp

The carrier densities and mobilities for electrons and holes of polycrystalline Bi samples from 50 K to 300 K were analyzed a two-carrier model without applying intrinsic conditions. Expressions of the transport coefficients for the analysis were obtained from the Boltzmann equation in the relaxation time and low magnetic field approximation assuming a value of the Fermi energies and a form for the scattering processes of each of the carriers. Two polycrystalline Bi samples were found to have different temperature dependent behaviors of the Seebeck coefficient. The difference of the carrier densities and the mobilities of the samples were quantitatively explained through the temperature dependent behaviors.

key words: carrier density, mobility, Boltzmann equation, relaxation time and low magnetic field approximation, scattering processes

1. INTRODUCTION

The performance of a thermoelectric material is expressed by the figure of merit Z, which is a function of the Seebeck coefficient α, resistivity ρ, and thermal conductivity κ [1]. The application of an external magnetic field enhances the figure of merit Z of Bi-based material more than twofold because the magneto-Seebeck coefficient under an optimum magnetic field under 0.5 Tesla, which is practically achievable in real applications, increases by a factor of 1.5 [2]. The magneto-Seebeck coefficient has been shown to be dependent on the shape of the sample, geometry effect, which is a disadvantage for bulk sample [3]. Therefore, Bi microwire array elements are fabricated such that enhance the magneto-Seebeck coefficient in enhanced by eliminating the geometry effect [4]. When a microwire array element is fabricated, the Bi is converted into polycrystalline Bi. Hence, the transport properties of polycrystalline Bi must be investigated from an analysis of carrier densities and the mobilities to improve of the performance of microwire array elements. In a past analysis of the transport properties of polycrystalline Bi using the quantitative mobility spectrum analysis (QMSA) procedure, the carrier densities and mobilities of electrons and holes were analyzed using expressions of the magnetic field dependence of the resistivity and the Hall coefficient without assuming intrinsic conditions [5]. However the magnetic field dependence of the resistivity and the Hall coefficient were measured in a strong magnetic field (7 Tesla). However, the QMSA procedure has a disadvantage in that the geometry effect not eliminated for high mobility samples such as Bi (the mobility μ_n of a single-crystal of Bi is 3.2×10^4 cm^2/Vs [6]) because the influence of the product of the mobility and magnetic field become large in the magnetic field dependence of the resistivity and Hall coefficient. To analyze the carrier density and the mobility accurately, the geometry effect should be eliminated. Hence, in this paper, the carrier densities and mobilities of electrons and holes of polycrystalline Bi samples were analyzed using expressions for the Seebeck coefficient, resistivity, magnetoresistance, and Hall coefficient. The resistivity, magnetoresistance, and Hall coefficient were measured by the Van der Pauw method in order to eliminate the geometry effect.

2. THEORY AND MODEL

The relaxation time τ_ε is proportional to r, the product of the ratio of the carrier energy ε to the average vibration of an atom [7]. The exponent r varies between -1/2 for acoustic deformation potential scattering and +3/2 for ionized impurity scattering. We consider a three-dimensional isotropic model to estimate the transport coefficients, namely the Seebeck coefficient α [8], resistivity in the absence of a magnetic field ρ_0 [7], magnetoresistance $\Delta\rho$ ($=\rho_B-\rho_0$, where ρ_B is the resistivity in a magnetic field satisfying the low magnetic field approximation) [7], and Hall coefficient R_H [7]. Each transport coefficient was obtained from the Boltzmann equation under a relaxation time and low magnetic field approximation, assuming a value of the Fermi energies and a form of the scattering processes of the carriers in a two-carrier model. Under this model the expression for the Seebeck coefficient is represented by an equation for nondegenerative materials and contains the index r and the Fermi Dirac integral $F_j(\eta)$ [8]:

$$F_j(\eta) = \frac{1}{j!}\int_0^\infty \frac{x^j}{\exp(x-\eta)+1}dx. \qquad (1)$$

where η is the reduced Fermi energy. We assumed that

the value of r was equal for electrons and holes so that the scattering process is the same for both carriers. In addition, the Hall factor r_H for the Hall coefficient was obtained from the definition.

$$r_H = \frac{\langle \tau_\varepsilon^2 \rangle}{\langle \tau_\varepsilon \rangle^2} = \frac{3\sqrt{\pi}}{4} \frac{\left(2r+\frac{3}{2}\right)!}{\left(\left(r+\frac{3}{2}\right)!\right)^2} \frac{F_{2r+\frac{1}{2}}(\eta) F_{\frac{1}{2}}(\eta)}{\left(F_{r+\frac{1}{2}}(\eta)\right)^2}. \quad (2)$$

In Ref. 7, the Hall factor r_H does not contain the Fermi Dirac Integral $F_j(\eta)$ because it was assumed for the reduced Fermi energy that $\eta < -4$, namely that Maxwell-Boltzmann statistics were applicable and the Fermi Dirac integral $F_j(\eta)$ could be approximated by $\exp(\eta)$. However, for the semimetal considered in this study, $\eta > 0$ and eq. (2) should be used for r_H of in this paper. The details of this analysis method are given in Ref. 9.

3. EXPERIMENTAL SETUP

Two polycrystalline Bi samples fabricated by a hot-press method were prepared for the measurement of the Seebeck coefficient, resistivity, magnetoresistance, and Hall coefficient. Table 1 describes the shape of both samples. For the measurement of the Seebeck coefficient, both ends of the samples were glued to Cu electrodes using low-resistivity Ag paste to stabilize the heat flux and to avoid chemical reactions with the Bi. Lead wires were attached to the Cu electrodes using conventional solder. Two calibrated Cernox temperature sensors were used to measure the temperature of the samples and were inserted into each Cu electrode. Heaters were attached to each Cu electrode to control the temperature using a two-loop feedback control system. For the measurement of the Seebeck coefficient, the thermoelectric voltage was measured four times for different temperature differences at temperatures from 50 K to 300 K. The Seebeck coefficient was estimated using a least squares method from the relationship between the temperature difference and the thermoelectric voltage to reduce the influence of the offset voltage. The resistivity, magnetoresistance, and Hall coefficient were measured by the Van der Pauw method to eliminate the geometry effect. The applied currents were quickly changed from ±I to ±2I, and then to ±3I, the voltage was measured for each current, and the resistance was calculated using a least squares method from the relationship between the current and the measured voltage to reduce the influence of the offset voltage and the thermoelectric voltage. For the measurements by Van der Pauw method, the magnetic field was satisfied the low magnetic field approximation.

Table I Shapes of samples A and B.

Geometry		Sample A	Sample B
for Seebeck coefficient measurement	Sample length [mm]	4.00	4.02
	Cross section [mm²]	2.00×1.85	2.00×2.01
for Van der Pauw method	Thickness [mm]	1.70	2.01
	Plane area [mm²]	10.05×10.10	10.03×10.01

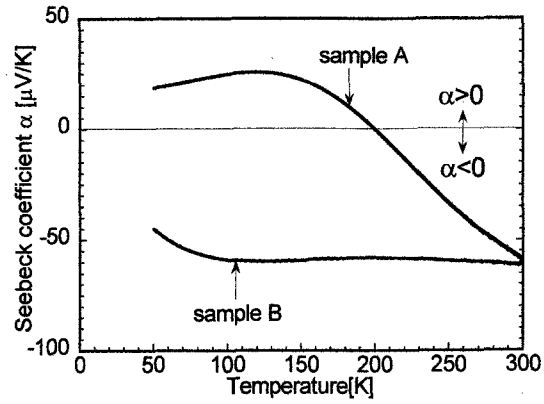

Fig. 1 Temperature dependence of the Seebeck coefficients from 50 K to 300 K

4. EXPERIMENTAL RESULT

Figure 1 shows the temperature dependence of the Seebeck coefficients for two samples. Both Seebeck coefficients are about -60 μV/K at 300 K and shows n-type transport properties. The Seebeck coefficient of sample A turns over to p-type at around 200 K as the temperature was decreases. The temperature dependence of the Seebeck coefficient below 200 K differs from that of single-crystal Bi, for which the sign of the Seebeck coefficient is known to be always negative [10]. Secondary-ion mass spectroscopy (SIMS) analysis indicated that Sn was the main impurity and approximately 0.01% was contained throughout sample A. On the other hand, the Seebeck coefficient of sample B was always negative, as that of single crystal Bi [10]. For the measurements of the resistivity, magnetoresistance, and Hall coefficient by the Van der Pauw method, the parameter f, which shows the error of the measurements and is close to 1 when the error is small, was more than 0.99 at all temperatures, and hence the error in the measurements was extremely small, showing that the measurements by the Van der Pauw method were made effectively. The magnitude of the magnetic field of sample A decreases with decreasing temperature and was 0.12 Tesla at 300 K and 6×10^{-4} Tesla at 50 K. It was smaller than that of sample B. Below 50 K, magnetoresistance could not be measured due to the small magnitude of the magnetic field, and therefore 50 K was the minimum temperature for our measurements.

5. ANALYSIS RESULT AND DISCUSSION

Calculation of the Seebeck coefficient and the Hall factor requires the values of the Fermi energy for each carrier. Since sample A contains about 0.01% Sn, the Fermi energies must be re-evaluated for the analysis. It has been reported that the Fermi energies of Sn-doped Bi containing about 0.02% Sn are 5 meV for electrons and 23 meV for holes [11]. This level of contained Sn is of the same order as that of sample A, and so we used these values for the Fermi energies of sample A. The Fermi energies of sample B were determined by calculations of the carrier densities and the mobilities, changing the value of the Fermi energies. We found that the temperature dependence of the carrier density of holes was similar to that of single crystal Bi when we assumed that the Fermi energies of sample B

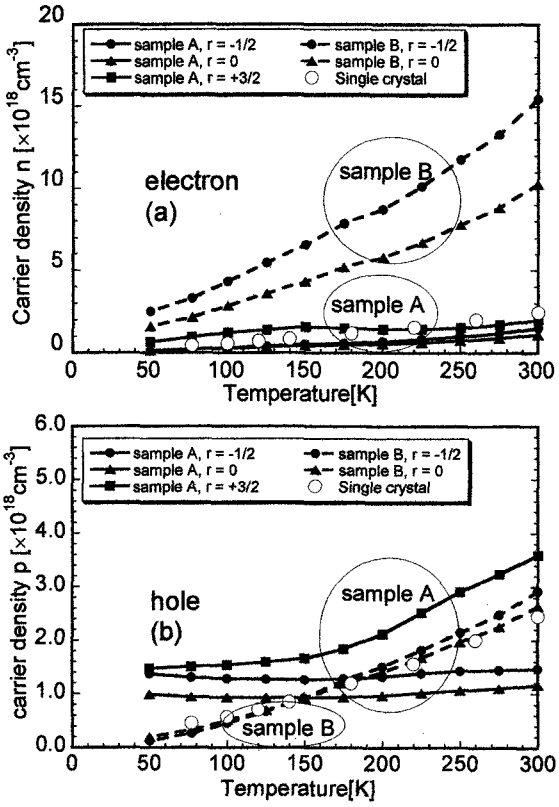

Fig.2 Calculated carrier densities as a function of temperature of (a) electrons and (b) holes. The open circles represent the averaged carrier densities for single-crystal Bi[2].

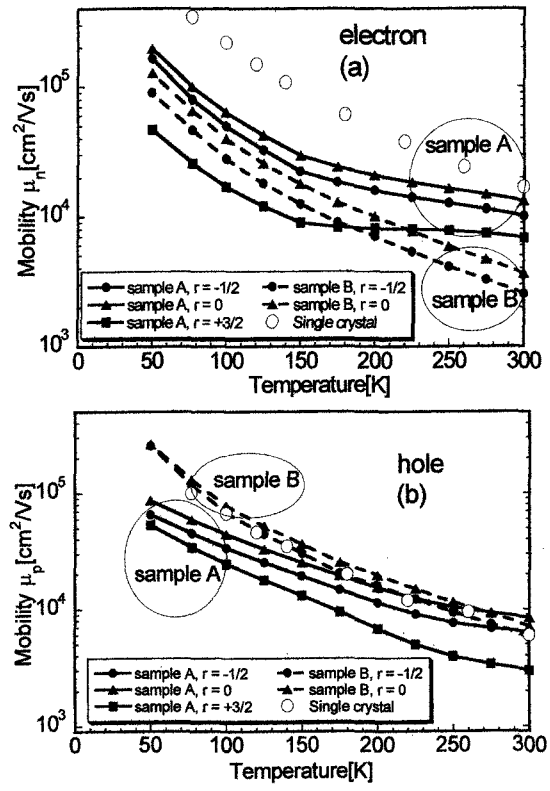

Fig.3 Calculated mobilities as a function of temperature of (a) electrons and (b) holes. The open circles represent the averaged mobilities for single-crystal Bi [2].

were 18 meV for electrons and 10 meV for holes, and hence we used these values [6]. In this analysis, we assumed a form of the scattering process, namely the value of r, the Seebeck coefficient, resistivity, magnetoresistance, and Hall coefficient were calculated assuming a value for r in the range $-1/2 < r < +3/2$ [7, 8], though for sample B was in the range of $-1/2 < r < 0$ because the Seebeck coefficient shifts downward in a magnetic field[8, 10]. Figures 2 and 3 show the calculation results of the carrier densities and the mobilities for electrons and holes using the experimental results of the Seebeck coefficient, resistivity, magnetoresistance, and Hall coefficient and assuming a value for r and a value of the Fermi energies. Figure 2 shows the calculated carrier densities for electrons and holes as a function of temperature. Since the relaxation time does not depend on the temperature, the carrier densities n and p have minimum values at $r = 0$ [7]. The temperature dependence of n of sample A agrees with the (arithmetic) averaged carrier density for the three axes of single-crystal Bi below 200 K [6]. A change in the temperature dependence of n due to the Sn in sample A could not be identified in Fig. 2(a). On the other hand, n of sample B increases with increasing temperature and is larger than the averaged carrier density of single-crystal Bi by a factor of 4 to 5 at all temperatures. However, a change in the temperature dependence of n due to ionization of impurities could not be identified in Fig. 2(a). Figure 2(b) shows that the temperature dependence of the carrier density for holes p of sample A differs from that of the averaged carrier density [6]. The rate of increase of p of sample A increases with an increase in the absolute value of r. Below 150 K, p is constant at about 1.0 to 1.5×10^{18} cm^{-3} and is larger than the averaged carrier density of single-crystal Bi. A comparison of p of sample A and the carrier density of single-crystal Bi, suggests the presence of an influence due to ionization of the Sn, and the temperature dependence of p is opposite to that of the n sample B. In past studies, the carrier densities of Te-doped Bi and Sn-doped Bi were found to be constant at low temperatures due to ionization of the impurities [13-15]. We compared our analysis results with those of Te-doped Bi because the temperature dependence of the carrier density of Sn-doped Bi has not been reported [14, 15]. For an amount of carriers from the Te of 1.5×10^{18} cm^{-3}, n was almost constant below 100 K because the Te was ionized, adding to the n of Bi [14]. At 2 K, the carriers from the Te are frozen-out and the ionization energy of Sn is smaller than that of Te [15,16]. Therefore, the Sn may ionize in sample A and act as an accepter above 50 K. The carrier density p of the Sn added to that of sample A and hence the p of the sample A is almost constant below 150 K, even though the carrier density of single-crystal Bi increases with increasing temperature. The p from Sn may be the dominant contribution to the p of sample A below 150 K. Hence, we must consider the value of p in detail. For an order of Sn doping of approximately 0.01% from the SIMS measurement, it was expected that the carrier density of donors N_D is about 10^{18} to 10^{19} cm^{-3} and the value of p

below 150 K of about 1.0 to 1.5×10^{18} cm^{-3} is valid. On the other hand, temperature dependence of p of sample B is similar to the carrier density of single-crystal Bi due to our assumption of Fermi energies [2].

Calculated mobilities for electrons and holes as a function of temperature are shown in Fig. 3. The mobilities μ_n and μ_p have a maximum value at $r = 0$ and decrease with increasing absolute value of r. The relaxation time is independent of temperature and the scattering process is not influenced by increasing temperature when $r = 0$ [7]. Figure 3(a) shows that the values of the mobility μ_n of sample A are different from the (arithmetic) averaged mobility of single-crystal Bi by a factor of 1/3 to 1/10 due to boundary scattering in polycrystalline Bi below 150 K[6]. The trend of the temperature dependence of μ_n does not change even as r is varied in the range $-1/2 < r < +3/2$.The value $|d\mu_n/dT|$ decreases with increasing temperature above 150 K, and the μ_n are different from the averaged mobility of single-crystal Bi by a factor of 2/3 to 1/3. The μ_n of sample B is also smaller than the averaged mobility of single-crystal Bi by a factor of 1/4 to 1/5 and smaller than that of sample A above 200 K. The value $|d\mu_n/dT|$ of sample B is constant at all temperatures. For sample B, the temperature dependence of the electric conductivity for electron σ_n is similar to that of single-crystal Bi due to the temperature dependence of μ_n, which is smaller than that of single-crystal Bi by a factor of 1/4 to 1/5 even though n of sample B is larger than that of single-crystal Bi by a factor of 4 to 5. Figure 3(b) shows that the difference between the mobility μ_p of sample A and the mobility of single-crystal Bi is smaller than that for μ_n, even though the carriers from Sn act as p-type carriers and there may be influences due to boundary scattering for polycrystalline Bi. The temperature dependence of the mobilities and the carrier densities of sample A indicates that the electric conductivity σ_p for holes is larger than σ_n for electrons, especially at low temperature. On the other hand, μ_p of sample B is similar to the averaged mobility of single-crystal Bi under the Fermi energies assumption, and σ_p of sample B is similar to that of single-crystal Bi due to the temperature dependence of μ_p as well as σ_n [6]. It is shown that the electric conductivities of sample B were similar to that of single-crystal Bi even if the increases in n due to impurities was larger than p of sample A. From this analysis, the temperature dependences of the carrier densities due to impurities and the mobilities due to boundary scattering were found to be the source of the temperature dependence of the electric conductivities.

6.CONCLUSION

The carrier densities and mobilities of polycrystalline Bi samples were successfully analyzed using expressions for the transport coefficients obtained from the Boltzmann equation in the relaxation time and low magnetic field approximation assuming a value of the Fermi energies and a form for the scattering processes of each carrier. It was shown that the temperature dependent behavior of the carrier densities and mobilities consistent with the past analysis result for single-crystal Bi. The temperature dependent behaviors of the electric conductivities were quantitatively explained using the temperature dependent behavior of the carrier densities and mobilities, which were influenced by impurities and boundary scatering, respectively.

ACKNOWLEDGEMENTS

The research was financially supported by the Sasakawa Scientific Research Grant from the Japan Science Society and was partly supported by the Industrial Technology Research Grant Program in '04 from the New Energy and Industrial Technology Development Organization (NEDO) of Japan, the Grant-in-Aid for Encouragement of Young Scientist from the Japan Society for the Promotion of Science, and the Murata Science Foundation. The authors would like to express their gratitude to Dr. T. Kobayashi in RIKEN for SIMS measurements.

REFERENCES

[1]G. S. Nolas, J. Sharp, and H. J. Goldsmid, *Thermoelectrics: Basic Principles and New Materials Developments* (Springer, Berlin, 2001) pp.91

[2] R. Wolfe and G. E. smith, Appl. phys. Lett. **1** (1962) pp.5-7

[3] D. R. Baker and J. P. Heremans, Phys. Rev. B. 59, (1999) pp.13927-13942

[4] Y. Hasegawa,Y. Ishikawa, T. Komine, T. E. Huber, A. Suzuki, H. Morita and H. Shirai, Appl. Phys. Lett. **85** (2004), pp. 917-919

[5]F. Brochin, B. Lenoir, C. Bellouard and H. Scherrer: Phys. Rev. B 63 (2001) pp. 073106-1 - 4

[6]J-P. Michenaud and J-P Issi, J. Phys. C: Solid State Phys. **5** (1972) pp.3061-3072

[7]For a review, K. Seeger, *Semiconducter physics*, 6th ed, (Springer Verlag, Berlin, 1988) pp. 38-59

[8]Y. Hasegawa, T. Komine, Y. Ishikawa, A. Suzuki, and H. Shirai, Jpn. J. Appl. Phys. **43** (2004), pp. 35-42

[9]Yoshiaki Ishikawa,Yasuhiro Hasegawa, Takashi Komine, Hiroyuki Morita, Hajime Shirai, Hiroaki Nakamura,Tetsuro Saso, Jpn. J. Appl Phys(submitted)

[10]C. G. Gallo, B. S. Chandrasekher, and P. H. Sutter, J. Appl. Phys. **34,** (1963) pp. 144-152

[11]R. T. Bate and N. G. Eispruch, Phys. Rev. **153** (1966) pp. 796-799

[12]T. C. Harman, Phys. Rev. **118** (1960) pp.1541-1542

[13]J. Heremans and O. P. Hansen, J. Phys. C: Solid State Phys. **16** 4623 (1983) pp.4623-4636

[14]J. Heremans, D. T. Morelli, D. L. Partin, C. H. Olk, C. M. Thrush, and T. A. Perry, Phys. Rev. B **38** 10280 (1988) pp. 10280-10284

[15]Yu-Ming Lin, Stephen B. Cronin, Jackie Y. Ying, and M. S. Dresselhaus, Appl. Phys. Lett. **76,** 3944 (2000) pp.3944-3946

[16]For a review, see C. Kittel, *Introduction to Solid State Physics*, 7th ed. (John Wiley and Sons, Inc., 1996) pp.67

(Received December 23, 2004; Accepted February 15, 2005)